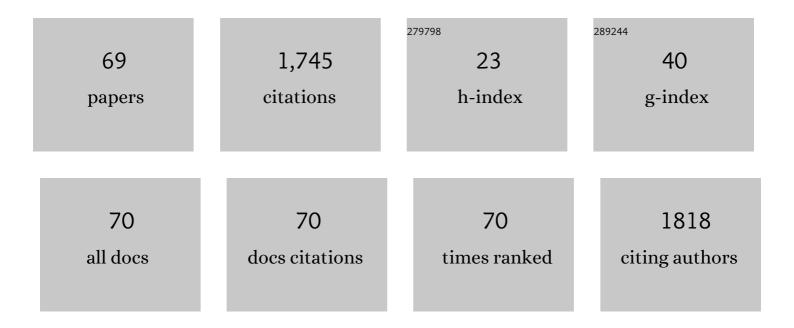
## Li-Kun Xu

List of Publications by Year in descending order

Source: https://exaly.com/author-pdf/922222/publications.pdf Version: 2024-02-01



#	Article	IF	CITATIONS
1	IrO <sub>2</sub> -Ta <sub>2</sub> O <sub>5</sub> Anode for Oxygen Evolution with TaO <sub>x</sub> Interlayer Prepared by Thermal Decomposition in Inert Atmosphere. Journal of the Electrochemical Society, 2022, 169, 046516.	2.9	2
2	Enhancement of corrosion resistance and lubricating performance of electrodeposited Ni-Co coating composited with mesoporous silica nanoparticles and silicone oil impregnation. Materials Chemistry and Physics, 2022, 282, 125929.	4.0	5
3	Performance of SS304 Modified by Silver Micro/Nano-Dendrite Coating with Hot-Water Super-Repellency in Simulated PEMFC Cathode Environment. Nanomaterials, 2022, 12, 1726.	4.1	2
4	Investigation of acidity on corrosion behavior and surface properties of SS304 in simulated PEMFC cathode environments. International Journal of Hydrogen Energy, 2022, 47, 22938-22951.	7.1	6
5	Properties of SS304 Modified by Nickel–Cobalt Alloy Coating with Cauliflower-Shaped Micro/Nano Structures in Simulated PEMFC Cathode Environment. Nanomaterials, 2022, 12, 1976.	4.1	4
6	Pitting corrosion of 2Cr13 stainless steel in deep-sea environment. Journal of Materials Science and Technology, 2021, 64, 187-194.	10.7	30
7	Impact of inhibitor loaded mesoporous silica nanoparticles on waterborne coating performance in various corrosive environments. Journal of Applied Polymer Science, 2021, 138, .	2.6	13
8	Corrosion resistance of a superhydrophobic dodecyltrimethoxysilane coating on magnesium alloy AZ31 fabricated by one-step electrodeposition. New Journal of Chemistry, 2021, 45, 14665-14676.	2.8	17
9	Corrosion Behavior of T2 and B30 Cu-Ni Alloy at Different Seawater Depths of the South China Sea. Journal of Materials Engineering and Performance, 2021, 30, 6027-6038.	2.5	7
10	Influence of temperature on corrosion behavior, wettability, and surface conductivity of 304 stainless steel in simulated cathode environment of proton exchange membrane fuel cells. International Journal of Hydrogen Energy, 2021, 46, 22920-22931.	7.1	19
11	Challenges and solutions of cathodic protection for marine ships. Corrosion Communications, 2021, 2, 33-40.	6.0	27
12	Peroxidase-like and oxidase-like nanozyme activities of reusable Mn–Co–S–Se/Ni foam for antibacterial application. Colloids and Surfaces A: Physicochemical and Engineering Aspects, 2021, 626, 127010.	4.7	5
13	Long-term corrosion behaviour of 1060 aluminium in deep-sea environment of South China Sea. Corrosion Engineering Science and Technology, 2021, 56, 327-340.	1.4	13
14	Identifying defect size in organic coatings by electrochemical noise, galvanostatic step and potentiostatic step techniques. Journal of Electroanalytical Chemistry, 2020, 856, 113596.	3.8	8
15	In situ study of the deep sea electrochemical performance of aluminumâ€based galvanic anodes. Materials and Corrosion - Werkstoffe Und Korrosion, 2020, 71, 1946-1956.	1.5	2
16	A Selfâ€Cleaning Mucusâ€like and Hierarchical Ciliary Bionic Surface for Marine Antifouling. Advanced Engineering Materials, 2020, 22, 1901198.	3.5	17
17	Fabrication of zinc-aluminum composite coating on stainless steel with long-term protection durability. Philosophical Magazine Letters, 2020, 100, 55-62.	1.2	2
18	Fabrication of an ultrathin 2D/2D C3N4/MoS2 heterojunction photocatalyst with enhanced photocatalytic performance. Journal of Alloys and Compounds, 2019, 808, 151681.	5.5	56

Lı-Ким Хи

#	Article	IF	CITATIONS
19	Correlation between Passivity Breakdown and Composition of Passive Film Formed on Alloy 690ÂStudied by Sputtering XPS and FIB-HRTEM. Journal of the Electrochemical Society, 2019, 166, C332-C344.	2.9	21
20	Long-term field exposure corrosion behavior investigation of 316L stainless steel in the deep sea environment. Ocean Engineering, 2019, 189, 106405.	4.3	44
21	Reliability of the estimation of uniform corrosion rate of Q235B steel under simulated marine atmospheric conditions by electrochemical noise (EN) analyses. Measurement: Journal of the International Measurement Confederation, 2019, 148, 106946.	5.0	16
22	Corrosion behaviour investigation of 460 low alloy steels exposed in the natural deep-sea environment. Corrosion Engineering Science and Technology, 2019, 54, 485-492.	1.4	15
23	Measuring the atmospheric corrosion of Q235B and T91 steels using gray value, wavelet analysis and fuzzy Kolmogorov–Sinai entropy. Anti-Corrosion Methods and Materials, 2019, 66, 621-630.	1.5	7
24	Fabrication of a novel g-C3N4/Carbon nanotubes/Ag3PO4 Z-scheme photocatalyst with enhanced photocatalytic performance. Materials Letters, 2019, 234, 183-186.	2.6	37
25	Identifying defect levels in organic coatings with electrochemical noise (EN) measured in Single Cell (SC) mode. Progress in Organic Coatings, 2019, 126, 53-61.	3.9	33
26	First-principle calculation of the electronic structures and optical properties of the metallic and nonmetallic elements-doped ZnO on the basis of photocatalysis. Physica B: Condensed Matter, 2019, 555, 53-60.	2.7	28
27	Highly enhanced photoelectrochemical cathodic protection performance of the preparation of magnesium oxides modified TiO2 nanotube arrays. Journal of Electroanalytical Chemistry, 2019, 834, 138-144.	3.8	19
28	Sensing corrosion within an artificial defect in organic coating using SECM. Sensors and Actuators B: Chemical, 2019, 280, 235-242.	7.8	41
29	Development of an electrochemical sensor and measuring the shelf life of tinplate cans. Measurement: Journal of the International Measurement Confederation, 2019, 134, 500-508.	5.0	10
30	Enhanced visible light-driven activity of TiO2 nanotube array photoanode co-sensitized by "green― AgInS2 photosensitizer and In2S3 buffer layer. Electrochimica Acta, 2018, 269, 429-440.	5.2	54
31	Enhanced visible-light-driven photocatalytic activities of 0D/1D heterojunction carbon quantum dot modified CdS nanowires. Chinese Journal of Catalysis, 2018, 39, 841-848.	14.0	38
32	High-strength double network hydrogels as potential materials for artificial 3D scaffold of cell migration in vitro. Colloids and Surfaces A: Physicochemical and Engineering Aspects, 2018, 549, 50-57.	4.7	12
33	Effectively enhanced photocatalytic hydrogen production performance of one-pot synthesized MoS2 clusters/CdS nanorod heterojunction material under visible light. Chemical Engineering Journal, 2018, 345, 404-413.	12.7	128
34	Effectively enhanced photocatalytic degradation performance of the Ag-modified porous ZnO nanorod photocatalyst. Journal of Materials Science: Materials in Electronics, 2018, 29, 9301-9311.	2.2	14
35	Corrosion Inhibition from Thiol Self-assembly Layer: A High Pressure Perspective. Journal Wuhan University of Technology, Materials Science Edition, 2018, 33, 1334-1343.	1.0	1
36	Corrosion Behavior of Q235 Steel Exposed in Deepwater of South China Sea. Journal of Materials Engineering and Performance, 2018, 27, 4489-4496.	2.5	31

LI-Kun Xu

#	Article	IF	CITATIONS
37	Pitting Corrosion of 10Ni8CrMoV High-Strength Steel Induced by a Potential Perturbation. Journal of Materials Engineering and Performance, 2018, 27, 5794-5802.	2.5	2
38	Electrochemical Behavior of Mg-Al-Zn-Ga Alloy as Anode Materials in 3.5Âwt.% NaCl Solution. Journal of Materials Engineering and Performance, 2018, 27, 5460-5469.	2.5	6
39	Free-standing, layered graphene monoliths for long-life supercapacitor. Chemical Engineering Journal, 2018, 350, 386-394.	12.7	67
40	Temperature dependence of passivity degradation on UNS N08800 in near neutral crevice chemistries containing thiosulphate. Corrosion Science, 2018, 140, 260-271.	6.6	24
41	Fabrication of Ag-modified porous ZnMgO nanorods with enhanced photocatalytic performance. Journal of Materials Science: Materials in Electronics, 2018, 29, 16962-16970.	2.2	2
42	Evolution of Calcareous Deposits and Passive Film on 304 Stainless Steel with Cathodic Polarization in Sea Water. Coatings, 2018, 8, 194.	2.6	5
43	Corrosion mechanism of copper immersed in ammonium sulfate solution. Materials and Corrosion - Werkstoffe Und Korrosion, 2018, 69, 1597-1608.	1.5	6
44	Synthesis and characterisation of composite nanoparticles of mesoporous silica loaded with inhibitor for corrosion protection of Cu-Zn alloy. Corrosion Science, 2017, 120, 139-147.	6.6	60
45	Service Lifetime Estimation of EPDM Rubber Based on Accelerated Aging Tests. Journal of Materials Engineering and Performance, 2017, 26, 1735-1740.	2.5	17
46	Enhanced Photoelectrochemical Cathodic Protection Performance of the Secondary Reduced Graphene Oxide Modified Graphitic Carbon Nitride. Journal of the Electrochemical Society, 2017, 164, C822-C830.	2.9	28
47	Enhanced performance of microbial fuel cell using carbon microspheres modified graphite anode. Energy Science and Engineering, 2017, 5, 217-225.	4.0	23
48	Enhanced photoelectrochemical performance of hydrogen-treated SrTiO3/TiO2 nanotube arrays heterojunction composite. Journal of Electroanalytical Chemistry, 2017, 807, 213-219.	3.8	19
49	Quantitative Determination of the Amount of Copper(I) Oxide in the Corrosion Products Formed on Copper by the Potassium Permanganate Titration Method. International Journal of Electrochemical Science, 2017, 12, 11556-11570.	1.3	2
50	Electrochemical Characterization on the Potential Dependent Stress Corrosion Cracking Mechanism of 10Ni8CrMoV High Strength Steel. ISIJ International, 2017, 57, 888-894.	1.4	2
51	Photoelectrochemical Cathodic Protection Induced from Nanoflower-Structured WO <sub>3</sub> Sensitized with CdS Nanoparticles. Journal of the Electrochemical Society, 2016, 163, C928-C936.	2.9	17
52	Investigation of aging behavior and mechanism of nitrile-butadiene rubber (NBR) in the accelerated thermal aging environment. Polymer Testing, 2016, 54, 59-66.	4.8	109
53	Preparation and corrosion resistance of ZnO/CeO <sub>2</sub> composite films. Surface Engineering, 2016, 32, 32-37.	2.2	8
54	Spatial resolution comparison of AC-SECM with SECM and their characterization of self-healing performance of hexamethylene diisocyanate trimer microcapsule coatings. Journal of Materials Chemistry A, 2015, 3, 5599-5607.	10.3	32

LI-Kun Xu

#	Article	IF	CITATIONS
55	Comparative Study on Kinetics of Chlorine Evolution Reaction for Ru-La-O Oxide Coatings. Wuji Cailiao Xuebao/Journal of Inorganic Materials, 2015, 30, 493.	1.3	0
56	Effect of electrolysis temperature on surface morphology and stability of Ti/RuO2–IrO2–SnO2anode. Materials Research Innovations, 2014, 18, S4-665-S4-668.	2.3	0
57	Self-healing mechanisms of water triggered smart coating in seawater. Journal of Materials Chemistry A, 2014, 2, 1914-1921.	10.3	93
58	Self-healing properties of protective coatings containing isophorone diisocyanate microcapsules on carbon steel surfaces. Corrosion Science, 2014, 80, 528-535.	6.6	95
59	Synthesis of isocyanate microcapsules and micromechanical behavior improvement of microcapsule shells by oxygen plasma treated carbon nanotubes. Journal of Materials Chemistry A, 2013, 1, 776-782.	10.3	46
60	A Superjunction Schottky Barrier Diode With Trench Metal–Oxide–Semiconductor Structure. IEEE Electron Device Letters, 2012, 33, 1744-1746.	3.9	9
61	Electrochemical Impedance Spectroscopy (EIS) Study of Ru-La Oxide Coatings in NaCl Solution. Acta Chimica Sinica, 2012, 70, 1166.	1.4	2
62	The Promotional Effect of Lanthanum Additive on the Apparent Electrocatalysis of Ti/(Ru,Ir)O <sub>X</sub> Electrode. Advanced Materials Research, 2011, 299-300, 596-599.	0.3	0
63	A comparative study on IrO2–Ta2O5 coated titanium electrodes prepared with different methods. Electrochimica Acta, 2009, 54, 1820-1825.	5.2	94
64	Microstructure and Electrochemical Properties of IrO[sub 2]-Ta[sub 2]O[sub 5]-Coated Titanium Anodes. Journal of the Electrochemical Society, 2003, 150, B254.	2.9	54
65	A study on the deactivation of an IrO2–Ta2O5 coated titanium anode. Corrosion Science, 2003, 45, 2729-2740.	6.6	90
66	Electrochemical Surface Characterization of IrO[sub 2]-Ta[sub 2]O[sub 5] Coated Titanium Electrodes in Na[sub 2]SO[sub 4] Solution. Journal of the Electrochemical Society, 2003, 150, B288.	2.9	43
67	Self-Healing Ability of Smart Coating for Anticorrosion of Reinforcing Steel. Applied Mechanics and Materials, 0, 357-360, 680-683.	0.2	2
68	The Deactivation Mechanism of RuO2-IrO2-SnO2/Ti Anodes Under Alternative Current Electrolysis Condition. , 0, , .		2
69	Self-healing performance of water triggered smart coating characterized by local electrochemical techniques. , 0, , .		Ο